ORIGINAL ARTICLE

lajss.org© Latin American Journal of Solids and Structures

www.lajss.org

Experimental Characterization of the Fatigue Life of Bolted Flange Connections in Wind Turbine Towers: Implications for Structural Integrity

Nisanur Isik[a]*, Fatih Alemdar[a]

[a] Yildiz Technical University, Department of Civil Engineering, 34040 Istanbul, Türkiye. Email: nisanur.isik@std.yildiz.edu.tr, falemdar@yildiz.edu.tr

* Corresponding author

https://doi.org/10.1590/1679-7825/e8997

Abstract

The experimental study investigates design parameters affecting the fatigue performance of bolted flange connections using accelerated laboratory tests at 60–70% of static capacity. Constant-amplitude loading R = 2 Hz was applied to large-diameter high-strength bolts (M36 and M39, Grade 8.8), considering variations in flange material S355 and SAE 1045, bolt size, and loading 5 mm eccentricity. M39 bolts showed statistically significant longer fatigue life than M36 bolts 8,579 vs. 5,395 cycles, p = 0.023. A 5 mm loading eccentricity reduced fatigue performance due to induced bending effects. While both flange materials showed comparable fatigue lives, the higher ductility of S355 provided improved damage progression control. Dynamic stiffness monitoring identified a three-stage degradation process, with critical reductions in final fatigue stages, indicating potential for early failure detection. Although accelerated tests do not predict absolute service life, results provide relative performance rankings and practical guidance for bolt selection and design of large-scale bolted structures, particularly wind turbine towers.

Keywords

Bolted flange connections, fatigue, load eccentricity, dynamic stiffness, accelerated testing.

Graphical abstract

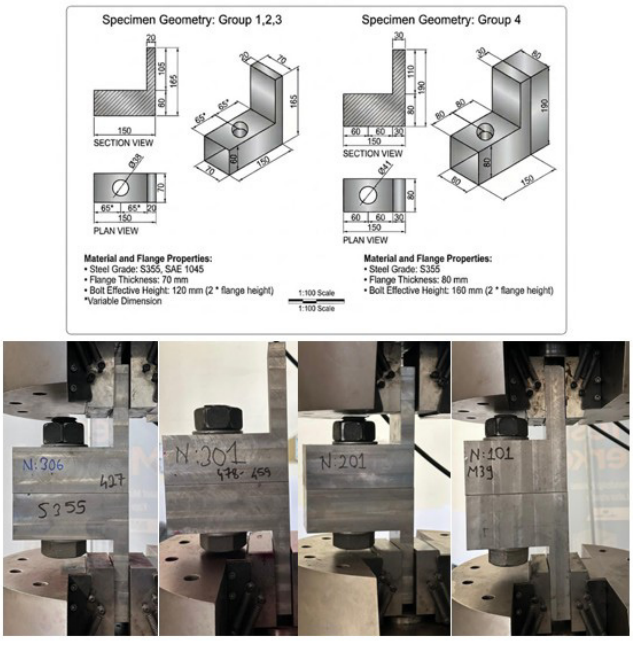

Received January 31, 2026. In revised form March 20, 2026. Accepted March 26, 2026. Available online March 30, 2026.
https://doi.org/10.1590/1679-7825/e8997

INTRODUCTION

Energy security and sustainability have emerged as paramount global challenges, driving a rapid transition from fossil fuels to renewable energy technologies. Wind energy has positioned itself as a fundamental pillar of this transition due to its technological maturity, economic competitiveness, and continuously improving efficiency. However, widespread wind turbine deployment has introduced complex engineering challenges related to operational reliability, service life optimization, and life cycle cost management.

Wind turbine towers experience multi axial, variable amplitude, high cycle loading throughout their operational lifetimes, typically designed for 20-25 years of service ($> 10^8$load cycles). Industrial failure reports demonstrate that a significant proportion of tower structural failures localize at flanged connection regions joining tower segments (Ma et al., 2018). The primary failure mechanism is fatigue crack development in flange bolts with subsequent propagation to critical size, resulting in catastrophic fracture.

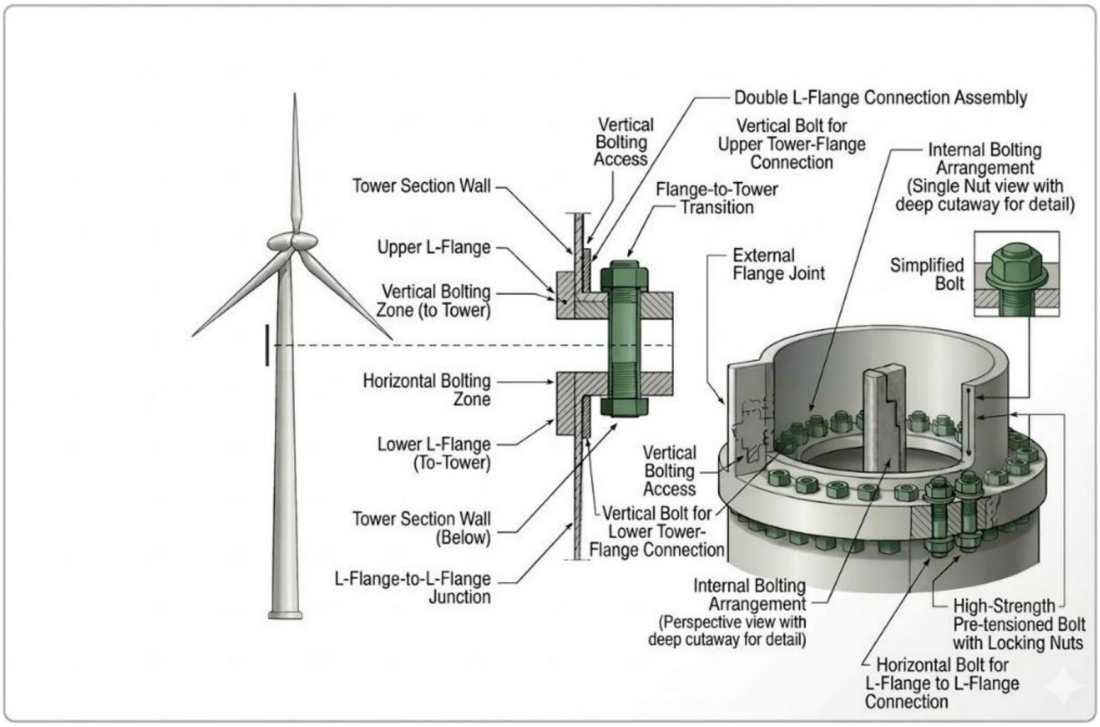

Figure 1 Location of bolted flange connections in a typical wind turbine tower and detail of the investigated connection geometry.

Figure 1 illustrates the structural context of this study, showing the location of bolted flange connections within a typical wind turbine tower and the detail of the connection geometry investigated experimentally.

1.1 Documented Failure Cases and Industrial Motivation

Globally documented incidents illustrate the recurrent nature of this problem. Table 1 summarizes critical wind turbine tower collapses attributed to bolted connection failures. These cases demonstrate that flange bolt design, assembly quality, and loading conditions play deterministic roles in structural integrity. Recent studies confirm that flange gaps and bolt fatigue critically affect connection stiffness, potentially causing structural collapse (Liao et al., 2019; Kim et al., 2025; Martínez-Vázquez et al., 2023). The mechanical behavior of bolted connections has been extensively investigated, with significant focus on preload loss mechanisms (Bickford, 2008; Chakherlou and Oskouei, 2011; Oskouei and Ibrahim, 2012), sealing performance (Aydın and Yılmaz, 2020; Oskouei et al., 2009; Pau et al., 2008), and fatigue life prediction models (Kim et al., 2025; Liao et al., 2019; Shao and Zhang, 2024). Finite element analysis (FEA) has enabled progress in understanding stress distribution and load transfer mechanisms (Aydın and Yılmaz, 2020; Cao and Zhang, 2019; Kumar et al., 2019). However, existing literature predominantly addresses general engineering applications, providing insufficient treatment of specialized requirements for mega-structures like wind turbine towers. Systematic parametric studies addressing fatigue the primary damage mode determining service life remain limited, revealing a distinct knowledge gap.

Table 1 Summary of Wind Turbine Tower Collapse Cases Due to Bolt Fatigue.

Year	Location	Turbine Model	Root Cause	Reference
2004	USA	1MW wind turbine	Bolt failure	(Alonso-Martinez et al., 2018)
2008	Denmark	Vestas V47 660kW	Bolt failure	(Alonso-Martinez et al., 2018)
2013	Japan	38 tonnes, 50m tower	Fatigue	(Alonso-Martinez et al., 2018)
2014	Germany	60m tower	Bolt failure	(Alonso-Martinez et al., 2018)

1.2 Research Gap and Motivation

Despite substantial progress in understanding bolted connection behavior, significant knowledge gaps persist in experimental characterization of large-diameter high-strength bolted connections. Previous studies have primarily focused on individual parameters in isolation:

Gap 1 - Limited Large-Diameter Bolt Data: Experimental fatigue data exist primarily for small-to-medium diameters M20-M30 (Zhou et al. (2022a); Ni et al., 2024; Yang and Lei, 2017; Shakeri et al., 2022; Zhou et al. (2022b)). Large-diameter bolts M36+ commonly specified in wind turbine applications lack sufficient experimental validation, with uncertain scalability of fatigue performance (Schaumann and Eichstädt, 2015; Lochana et al., 2019).

Gap 2 - Load Eccentricity Effects: Controlled experimental quantification of load eccentricity effects on fatigue life remains scarce, despite known prevalence of geometric imperfections and assembly tolerances in field installations (Ma et al., 2018; Liao et al., 2019). The dose-response relationship between eccentricity magnitude and fatigue degradation has not been systematically established.

Gap 3 Flange Material Property Influence: Systematic comparison of flange material properties ductility versus strength and their influence on connection fatigue performance and dominant failure modes has not been adequately established through physical testing. The interaction between flange ductility and progressive damage accumulation requires experimental clarification. Key Assessment: Gaps 1 and 2 are identified as highest priority for design practice, as they directly affect component selection (bolt sizing) and assembly quality control procedures. Gap 3, while important for understanding failure mechanisms, has secondary impact on fatigue life prediction based on preliminary literature review.

1.3 Research Objectives and Experimental Approach

This investigation addresses these gaps through a parametric experimental program that directly compares M36 versus M39 high-strength bolt performance under identical loading conditions to quantify scalability effects, quantifies the effect of load eccentricity on fatigue life to establish assembly tolerance requirements, and evaluates S355 structural steel high ductility, 18–19% elongation versus SAE 1045 carbon steel high strength, 7–9% elongation for flange fabrication to assess material property influence on damage progression.

The 5 mm eccentricity selected for this study reflects realistic assembly conditions inherent to bolted flange connections in grid structures. During fabrication and field installation, cumulative positional deviations in bolt-hole alignment and flange seating are unavoidable. EN 1090-2 Table D.2.8 defines functional manufacturing tolerances for fastener hole positions in structural steel assemblies; for bolt diameters in the M36–M39 range, such deviations at the flange interface can realistically produce load path offsets on the order of 3–6 mm. A 5 mm eccentricity therefore represents a conservative mid-range value within the permissible tolerance band, corresponding to conditions that may arise in compliant fabrication without exceeding normative limits. Prior experimental studies have demonstrated that even modest load eccentricity introduces supplementary bending stresses at the thread root, measurably reducing fatigue life relative to concentric loading (Zhou et al. (2022a); Zhou et al. (2022b); Ni et al., 2024). Quantifying this effect under controlled conditions is therefore essential for translating laboratory results into assembly tolerance requirements relevant to design practice.

Static tensile tests (Isik and Alemdar, 2025) established that single-nut configurations reach 220 kN with thread stripping failure, while double-nut configurations achieve 380–390 kN with stable performance up to 410 kN. Based on these reference values, the experimental program employs accelerated testing at 60–70% of static capacity 230 kN maximum load to enable comparative parametric assessment within practical laboratory timeframes. This approach intentionally produces low-cycle fatigue lives rather than the operational high-cycle lives 10^6–10^7 range expected in service. The primary objective is systematic quantification of relative performance differences among design parameters rather than absolute life prediction. Fatigue life exhibits power-law dependence on stress amplitude $N \propto \Delta\sigma^{-m}$, $m \approx 3$–5 meaning rank ordering and relative performance ratios observed at elevated stress remain valid indicators of comparative behavior at operational stresses. Translation to operational conditions requires validated computational models incorporating site-specific load spectra, appropriate damage accumulation theories (Zhou et al. (2022a); Ni et al., 2024), and adequate safety factors a two stage approach representing established best practice in structural fatigue

research. Dynamic stiffness monitoring throughout testing provides insights into progressive damage accumulation, with potential applications for structural health monitoring SHM system development.

1.4 Research Phases and Paper Organization

The research program consists of four phases. The first phase characterized the mechanical properties of S355 and SAE 1045 steels through tensile testing on dogbone specimens (ASTM E8), and the second phase determined the static load carrying capacity of single and double nut configurations, together providing the material and mechanical baselines described in Section 1.3 (Isik and Alemdar, 2025). Phases I and II are fully reported in that prior work and are not repeated here; the original contribution of the present paper comprises Phases III and IV. The third phase comprised the systematic constant-amplitude fatigue experiments across the four parametric groups. The fourth phase performed disaggregated analysis of the three important parameters loading eccentricity, flange material grade, and bolt strength grade with a minimum of three specimens per configuration to ensure statistical reliability and data reproducibility.

1.5 Expected Contributions

This comprehensive experimental database is expected to yield significant insights for both academic researchers and industrial practitioners: quantitative design guidance providing data-driven framework for bolt size selection, assembly tolerance specification, and material property requirements; FEM validation database as reference data for calibrating and validating computational models of large-diameter bolted connections; assembly quality standards with evidence-based recommendations for preload application and geometric tolerance control; and SHM algorithm development through stiffness degradation patterns for early warning system design.

The ultimate objective is contributing to more reliable, durable, and economical connection designs that extend wind turbine operational life, minimize maintenance costs, and improve the levelized cost of energy LCOE while supporting refinement of international standards EN 1993-1-9, DNV-GL, ISO 898-1.

2 RELATED WORK

The structural integrity of bolted flange connections in wind turbine towers is critically important due to the exposure of these joints to complex, high-cycle fatigue loads originating from operational and environmental effects. Connection failures, typically initiated by progressive bolt fracture or flange separation, can lead to gradual stiffness degradation and ultimately catastrophic structural collapse. Consequently, research in this domain has been structured to address two closely interconnected fundamental challenges: understanding the system-level behavior of flange connections under environmental conditions and accurately predicting the fatigue life of high-strength bolts. The general consensus in the literature emphasizes the critical importance of experimental data in bridging the gap between theoretical models with accompanying simulations and actual structural performance, particularly for large-diameter bolts commonly employed in turbine design.

Fundamental research has systematically investigated parameters affecting bolt fatigue. The detrimental effect of stress concentration in the thread root region the primary damage location has typically been analyzed through integrated application of experimental testing and finite element analysis (FEA) (Zhou et al. (2022a); Zhou et al. (2022b); Ni et al., 2024). While constant-amplitude tests provide fundamental S-N curves (Yang and Lei, 2017; Shakeri et al., 2022), they remain insufficient for predicting service life under complex loading regimes. Experimental studies have constituted important data sources for validating damage accumulation models and have consistently demonstrated that nonlinear cumulative damage theories such as Corten-Dolan exhibit superior accuracy compared to Miner's linear rule, as they better account for load sequence effects in constant-amplitude loading (Zhou et al. (2022a);2022b Ni et al., 2024).

In the study conducted by Johansen and Waldeland (2016), the behavior of bolt-nut assemblies under tensile force was comprehensively characterized through a combination of experimental and numerical methods. The study parametrically investigated the effect of nut position on damage modes occurring particularly at short and long grip lengths. Experimental findings revealed that thread stripping emerged as the dominant damage mode at short grip lengths, while ductile bolt fracture predominated at long grip lengths. Furthermore, it was quantitatively determined that positioning the nut close to the unthreaded region increased the risk of thread stripping, whereas high-nut geometry or double-nut usage ensured bolt fracture in all positioning scenarios.

In their research, Grimsmo et al. (2016) emphasized that thread failures experienced by bolt and nut assemblies under tensile loading are generally undesirable. Such failures exhibit a less ductile failure mode than fracture of the bolt's threaded shank. Due to the difficulty of detecting thread damage during assembly resulting from overtightening, the root causes of thread failures were systematically investigated. Thread stripping was observed to occur particularly when the Lt parameter (screw length within grip) was short. Thread failure occurred when Lt ≤ 9 mm, whereas bolt fracture occurred when $L_t \geq 17mm$.

In the study conducted by Plaitano et al. (2022), the failure behaviors of high-strength HV bolts were experimentally investigated not only under tension but also under combined tension and bending. Findings demonstrated that thread stripping was the dominant failure mode under pure tensile loading, whereas bolt shank fracture predominated under combined tension and bending.

The scalability of fatigue performance to large-diameter bolts (M36 and above) required for wind energy applications remains a critical research frontier. Schaumann and Eichstädt (2015) directly addressed the lack of experimental validation for bolts exceeding M36, quantitatively measured the significant effect of hot-dip galvanizing on fatigue performance, and experimentally validated design data for the S-N curve in EN 1993-1-9. This experimental gap for large-scale bolts represents a recurring theme in the literature, identified as a major source of uncertainty in current design standards (Lochana et al., 2019). Complementarily, the simulation-based study by Salameh et al. (2025) presents a systematic framework for optimizing bolt size and quantity, proposing that increasing bolt diameter may be as effective as adding a significant number of smaller bolts; this finding underscores the need for experimental validation of such optimization strategies.

A parallel research line has focused on the system-level response of complete turbine tower flange connections. Van-Long et al. (2013) conducted pioneering experimental tests on bolted flange connections for tubular structures, revealing critical discrepancies between standardized design predictions and experimental results. Their work demonstrated that system-level factors such as flange geometric imperfections and weld details can accelerate damage modes not captured by simplified analytical approaches. Using FE models, Seidel and Schaumann (2021) validated that geometric imperfections significantly alter load transfer and bolt forces. Another investigation by Alonso-Martinez et al. (2018) on turbine tower flange components revealed through post-mortem analysis of a collapsed turbine that failure resulted from insufficient material toughness in the flange, emphasizing that bolt performance is closely interrelated with the integrity of all connected components.

The interaction between connection design and bolt fatigue is a critical consideration. Pavlovic et al. (2015) compared conventional ring flange connections with friction-type connections, demonstrating that the latter offers superior fatigue performance for bolts due to significantly lower operational force ranges. This indicates that system-level connection selection directly determines component-level fatigue life. Furthermore, the effect of manufacturing and assembly quality represents another critical consideration. Casado et al. (2022) and Shakeri et al. (2022) experimentally demonstrated that factors such as preload, nut positioning, and thread imperfections can significantly alter fatigue life, emphasizing that laboratory idealizations can differ markedly from the operational behavior of actual fasteners.

In summary, fatigue assessment of wind turbine tower flange connections requires integrated understanding of connection behavior, local bolt fatigue, and environmental effects. Despite considerable progress through experimental and simulation approaches, high-quality experimental data for large-diameter bolts remain critically needed to validate models and optimize design. The present study addresses this gap through systematic parametric testing of M36 and M39 bolts under controlled laboratory conditions.

3 MATERIALS AND METHODS

3.1 Materials and Specimen Design

Joint specimens were manufactured from two distinct steel grades widely employed in structural applications: S355 structural steel and SAE/AISI 1045 carbon steel. Material selection was based on contrasting mechanical properties to evaluate the influence of strength-ductility trade-offs on connection fatigue performance. Mechanical properties were characterized through tensile tests on dogbone specimens in accordance with ASTM E8 standard in our previous work (Isik and Alemdar, 2025). The present study builds on those material and static capacity baselines to investigate fatigue behavior under cyclic loading, which was not addressed in that prior work.

S355 exhibited ductile fracture with progressive necking, while SAE 1045 displayed 30% higher strength but brittle fracture with minimal plastic deformation (Isik and Alemdar, 2025). High-strength bolts (M36 and M39, ISO 898-1, Grade 8.8) were employed, with M39 providing approximately 19% greater cross-sectional area 976 mm^2 vs. 817 mm^2 respectively.

3.2 Specimen Geometry and Design Rationale

An L-shaped flange geometry with connecting bolt was designed based on the 27-meter level flange connection of an 85-meter wind turbine tower (Seidel and Schaumann, 2021), scaled for laboratory testing. Key dimensions included flange of 150 mm width × 165-190 mm height × 70-80 mm thickness, bolt holes of Ø38 mm M36 or Ø41 mm M39, and clearance of 2 mm nominal ISO tolerance H13.

The L-shaped configuration enables pure tensile loading on the fastener while maintaining representative flange bending stiffness. Flange thickness was selected to prevent flange failure prior to bolt failure under design loads. The test

configuration was designed to apply predominantly axial tensile loading to the bolt, consistent with the dominant load transfer mechanism in wind turbine tower flange connections. In ring flange connections, the primary bolt loading arises from axial forces and bending moments acting on the tower cross-section, which are transferred to the bolts as tensile forces. Shear forces acting parallel to the flange interface are resisted by friction between the contact surfaces and do not directly load the bolts in shear under normal operating conditions (Van-Long et al., 2013; Seidel and Schaumann, 2021). Consequently, shear effects on bolt fatigue are considered negligible in the present configuration, and the axial tensile loading applied in this study represents the critical design loading condition. Figure 2 presents the technical drawing and Figure 3 shows manufactured specimens.

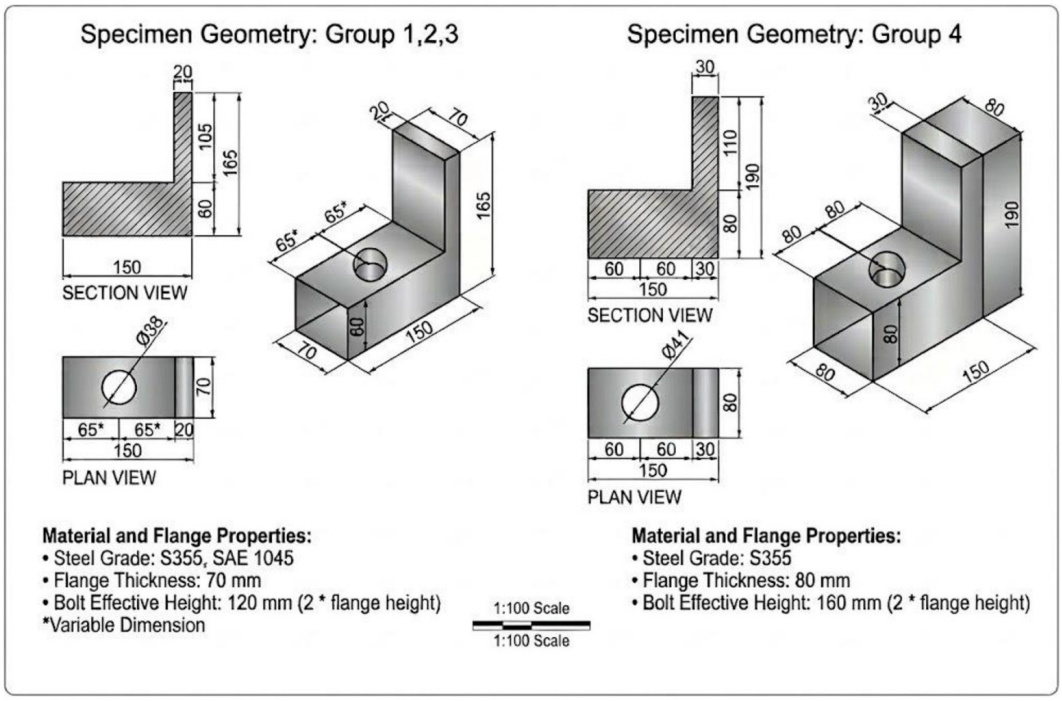

Figure 2 Technical drawing and dimensions of flange specimens.

Table 2 Summary of Specimen Sizes

Parameter	Group 1 & 2 & 3 (S355,M36)	Group 4 (S355,M39)
Width (mm)	150	150
Height (mm)	165	150
Thickness (mm)	20	30
Bolt hole (mm)	38	41
Clerance (mm)	2	2

The experimental progression consisted of four main groups: Group 1 (specimens 301-302-303, SAE 1045 flange material, M36 bolt), Group 2 (specimens 201-202-203, S355 flange material, M36 bolt, eccentric loading), Group 3 (specimens 304-305-306, S355 flange material, M36 bolt, centric loading), and Group 4 (specimens 101-102-103, S355 flange material, M39 bolt, centric loading).

3.3 Static Tensile Tests and Load Capacity Determination

Preliminary static tensile tests established ultimate load-carrying capacity and informed fatigue load selection, as reported in detail in Isik and Alemdar (2025). Those static tests constitute a distinct prior contribution; the present work utilizes the resulting capacity values solely to define the fatigue test load levels. Single-nut configurations achieved 221 ± 3 kN with thread stripping failure, while double-nut configurations reached 385 ± 5 kN with bolt shank fracture. Based on these results, fatigue testing employed 230 kN maximum load, approximately 60-65% of static capacity, sufficiently high to induce measurable fatigue damage within practical test duration while avoiding thread stripping. Single-nut configuration was

selected for fatigue tests as it exhibited similar yield behavior to double-nut systems and represents common industrial practice.

Figure 3 Manufactured flange specimens.

Table 3 Experimental test group configurations.

Test Group	Specimen Numbers	Flange Material	Bolt Size	Loading Condition
Group 1	301-302-303	SAE 1045	M36	Centric
Group 2	201-202-203	S355	M36	Eccentric (5 mm)
Group 3	304-305-306	S355	M36	Centric
Group 4	101-102-103	S355	M39	Centric

3.4 Test Setup and Equipment

All tests were performed using an Instron 8801 servo-hydraulic testing system ±250 kN capacity, ±75 mm displacement, load accuracy ±0.5%, displacement accuracy ±0.1%. Specimens were mounted axially between hydraulic grips using custom adapter plates. For eccentric loading tests Group 2, a specially designed offset fixture introduced 5 mm lateral displacement of the loading axis. Alignment was verified using digital calipers and laser alignment accuracy ±0.1 mm.

3.5 Assembly Procedure and Preload Application

Bolt connections were assembled following standardized procedure to minimize variability surface preparation with flange surfaces cleaned with acetone and inspected bolt insertion with bolt inserted with washer placed under nut hand tightening with nut hand-tightened to ensure full thread engagement torque application using calibrated digital torque wrench accuracy ±2% with specified torque of M36 450 Nm and M39 520 Nm; and verification by torque re-checked after 5-minute relaxation period.

Preload Estimation: For M36 bolt at 450 Nm: $F = \frac{T}{Kxd} \approx \frac{450}{0.2x0.036} = 62.5$ (1), representing approximately 12% of proof load (523 kN). This is lower than the ISO 16047 target of 70% due to friction coefficient uncertainty in the K×d relationship. Actual preload may vary ±20%. This limitation is acknowledged; future work should employ ultrasonic bolt tension measurement for precise preload verification.

3.6 Fatigue Testing Protocol

Constant-amplitude sinusoidal loading was applied with the following parameters: maximum load of 230 kN, minimum load of 23 kN, load ratio $R = \frac{Pmax}{Pmin} = 0.1$ (2) frequency of 2 Hz, and waveform as sinusoidal tension-tension.

The following parameters were continuously recorded at 100 Hz throughout each test applied load (kN), crosshead displacement (mm), cycle count, and dynamic stiffness calculated as $K = \Delta F/\Delta\delta$ (3) for each cycle. Progressive stiffness reduction indicates accumulating damage.

Tests were continued until one of the following conditions was met unable to sustain minimum load 23 kN, crosshead displacement exceeds 50 mm, or audible crack with visible separation.

3.7 Statistical Analysis

Statistical methods employed included descriptive statistics with mean fatigue life, standard deviation (SD), coefficient of variation $CoV = \frac{SD}{Mean} x100\%$ (4) and inferential statistics with two-tailed Student's t-test for pairwise comparisons (n≥3), significance level α = 0.05 (95% confidence), and confidence intervals calculated for each group mean.

Data Quality and Outlier Assessment included visual inspection of data consistency within each test group, protocol compliance verification load level, assembly procedure, test conditions, deviation analysis from expected behavior based on theoretical models, and specimens exhibiting protocol violations were excluded from statistical analysis.

Sample Size Justification: Minimum n=3 specimens per group provides sufficient data for mean and standard deviation estimation with capability to detect large effect sizes Cohen's d > 1.5. While larger samples n≥5 would improve statistical power, n=3 represents a practical balance between experimental resource constraints and preliminary comparative assessment. All statistical calculations were performed using Microsoft Excel with Data Analysis ToolPak. Importantly, fatigue life assessment is conducted on a logarithmic scale, as fatigue life follows a log-normal distribution (Yang and Lei, 2017; Zhou et al. (2022a)). On this scale, cycle counts of 7,200 and 7,300 which appear numerically distinct differ by only log(7300/7200) ≈ 0.006 log-units, a negligible difference relative to the observed group separation of approximately 0.20 log-units between M36 and M39 groups. Consequently, even if additional specimens were to shift the mean modestly, the relative performance rankings and the statistical significance of the primary finding M39 vs. M36, p=0.023, Cohen's d=2.18 would remain robust.

4 EXPERIMENTAL RESULTS

4.1 Overview of Fatigue Life Results

Fatigue test results from four parametric groups are summarized in Table 4. Results demostrate that bolt diameter, loading eccentricity, and flange material exert measurable effects on fatigue life, with bolt size showing the most pronounced influence.

Table 4 Summary of fatigue test results

Specimen	Test Group	Flange Material	Bolt	Loading	$Log_{10}(N)$	Max. Load (kN)	Failure Mode
N:101	Group 4	S355	M39	Centric	3,976	229,95	Bolt shank
N:102	Group 4	S355	M39	Centric	3,96	229,12	Bolt shank
N:103	Group 4	S355	M39	Centric	3,854	229,94	Bolt shank
N:304	Group 3	S355	M36	Centric	3,344	268,75	Premature failure
N:306	Group 3	S355	M36	Centric	3,772	230,11	Bolt shank
N:301	Group 1	SAE 1045	M36	Centric	3,739	230,14	Bolt shank
N:302	Group 1	SAE 1045	M36	Centric	3,659	230,19	Bolt shank
N:303	Group 1	SAE 1045	M36	Centric	3,787	230,19	Bolt shank
N:201	Group 2	S355	M36	Eccentric	3,741	230,08	Flange + Bolt
N:202	Group 2	S355	M36	Eccentric	3,834	230,04	Bolt shank
N:203	Group 2	S355	M36	Eccentric	3,675	230,14	Flange + Bolt

Specimen N:304 was excluded from statistical analysis due to premature failure at elevated load level (268.75 kN).

Table 5 Statistical summary of fatigue test results.

Test Group	Material	Bolt	n	Number of Cycles	Std Dev	CoV (%)	Min-Max	95% CI
Group 4	S355	M39	3	8,579	1,211	14,1	7,151-9,461	±1,394
Group 1	SAE 1045	M36	3	5,395	791	14,7	4,566-6,130	±911
Group 2	S355	M36	3	5,694	1,05	18,4	4,738-6,826	±1,209
Group 3	S355	M36	1	5,916	-	-	-	-

Group 3: n=1 after exclusion of N:304 as outlier.

Key Performance Rankings:

M39 bolts (Group 4): 8,579 ± 1,211 cycles (highest performance)

M36 eccentric (Group 2): 5,694 ± 1,050 cycles

M36 baseline S355 (Group 3): 5,916 cycles (single specimen)

M36 SAE 1045 (Group 1): 5,395 ± 791 cycles

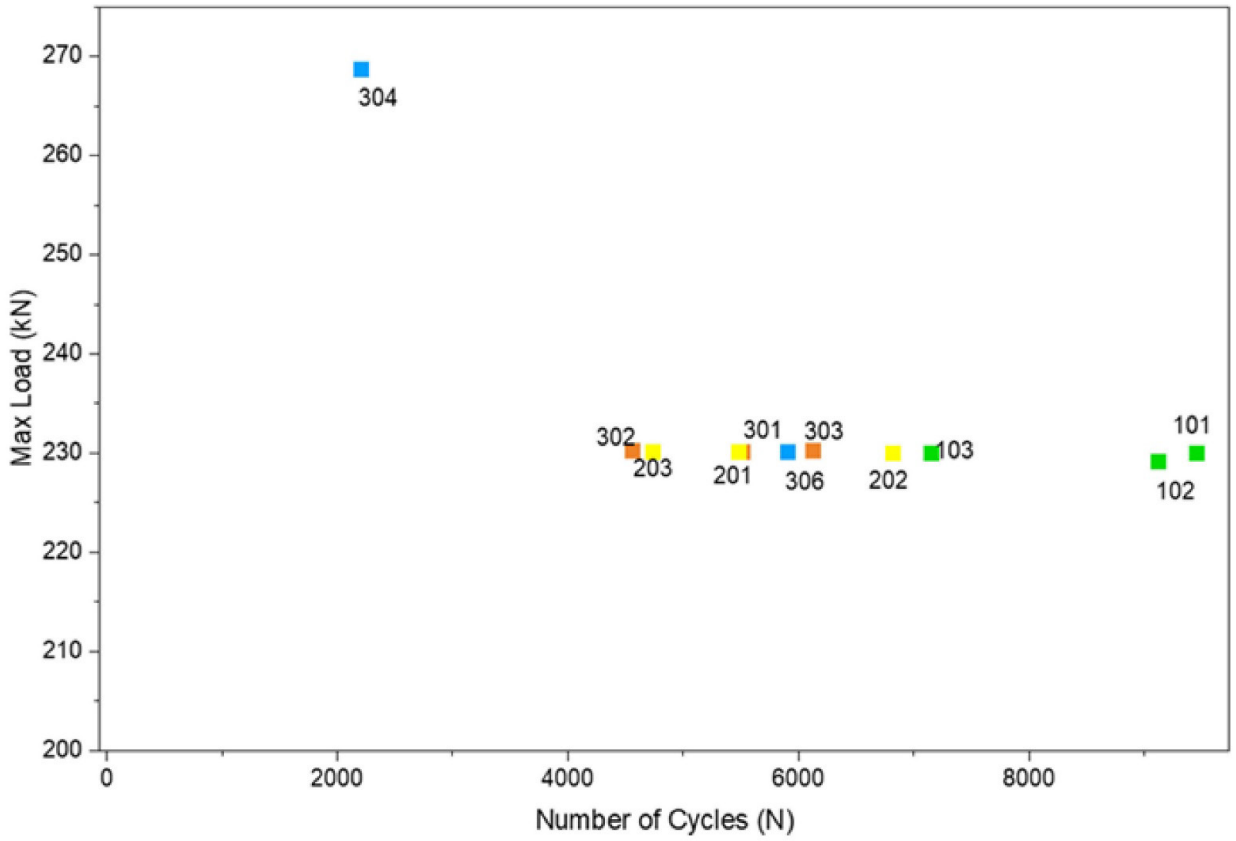

Figure 4 Fatigue life comparison graph.

4.1.1 Statistical Outlier Analysis - Specimen N:304

Specimen N:304 exhibited anomalously low fatigue life 2,208 cycles at elevated load 268.75 kN vs. target 230 kN, representing a 16.8% protocol deviation. Assuming power-law relationship $N \propto \Delta\delta^{-m}$ with m=3.5, the expected life at 268.75 kN would be approximately 3,850 cycles, yet observed life was only 2,208 cycles 57% of expected, suggesting compound effects of load error and potential material or assembly irregularities. N:304 was excluded due to protocol non-compliance, reducing Group 3 to a single valid specimen N:306 and precluding statistical comparison of flange materials. The load deviation was confirmed through review of the recorded test data, which showed a consistent offset from the target load throughout the test duration. Post-test visual inspection of the fracture surface revealed morphology consistent with other specimens in the group, suggesting no atypical material or assembly anomaly. The exclusion is therefore attributed to load protocol non-compliance rather than an inherent specimen defect.

4.1.2 Statistical Comparison of Test Groups

Pairwise t-test comparing Group 4 M39 vs. Combined M36 Groups (1+2): Group 4 mean of 8,579 cycles, combined M36 mean of 5,545 cycles (n=6), difference of 3,034 cycles 54.7% improvement, two-tailed t-test p = 0.023. Conclusion: M39 bolts exhibit statistically significant superior fatigue life (α = 0.05).

Comparison of Group 1 SAE 1045 vs. Group 2 S355 eccentric: difference of 299 cycles 5.5%, two-tailed t-test p = 0.66. Conclusion: No statistically significant difference.

Coefficients of variation 14.1-18.4% fall within acceptable ranges for fatigue testing. Group 2 (eccentric loading) exhibited highest CoV 18.4%, reflecting additional scatter from load path irregularities.

4.2 Effect of Bolt Diameter and Strength Grade

M39 high-strength bolts Group 4 demonstrated substantial performance advantage over M36 bolts Groups 1-3, with statistically significant improvement in mean fatigue life ($p=0.023$) and Cohen's $d = 2.18$ very large effect. Pre- and post-test specimen appearances are shown in Figures 5-6, with dynamic stiffness data presented in Section 4.5.

The comparative analysis of SAE 1045 steel indicates that M39 consistently outperforms M36 in terms of fatigue endurance. Experimental data for M39 exhibited a performance range between 7,151 cycles and 9,461 cycles.Notably, even the lower bound of the M39 dataset surpassed the peak performance of M36 by a margin of 17%, demonstrating a robust enhancement in material longevity regardless of sample variance.

All M39 specimens exhibited classic bolt shank fatigue fracture with crack initiation at thread root region, progressive crack growth evidenced by beach marks, and final rapid fracture zone occupying 30-40% of cross-section. No thread stripping or nut damage was observed.

Figure 5 Pre-fatigue test appearance of N101, N102, N103 specimens with M39 bolts.

Figure 6 Post-fatigue test appearance of N101, N102, N103 specimens with M39 bolts.

4.3 Effect of Flange Material Grade

Direct comparison between SAE 1045 Group 1 and S355 Group 3 flange materials was limited by exclusion of N:304, reducing Group 3 to a single valid specimen. SAE 1045 mean Group 1 yielded 5,395 ± 791 cycles while S355 single specimen N:306 produced 5,916 cycles a difference of 521 cycles 9.6%. The S355 specimen falls within the confidence interval of SAE 1045 group 4,484-6,306 cycles, suggesting similar fatigue life for both materials under tested conditions.

Despite similar fatigue lives, post-test examination revealed distinct damage progression patterns between the two flange materials. These observations align with fundamental fracture mechanics principles and material ductility effects documented in structural steel research.

SAE 1045 carbon steel (high strength, low ductility) exhibited characteristic brittle fracture behavior with sharp, clean fracture surfaces showing minimal plastic deformation, limited flange bending with elastic-dominated response, and multiple sharp radial cracks propagating from bolt holes with minimal crack tip blunting. The 7-9% elongation capacity (Isik and Alemdar, 2025) resulted in limited energy dissipation prior to final fracture, consistent with brittle failure modes observed in high-strength, low-ductility steels under cyclic loading (Grimsmo et al., 2016; Plaitano et al., 2022).

In contrast, S355 structural steel (moderate strength, high ductility**)** displayed ductile fracture characteristics including more diffuse fracture surfaces with evidence of substantial plastic deformation, noticeable flange bending and yielding concentrated near the bolt hole region, and fewer but wider cracks with visible plastic zone development around crack tips. The superior 18-19% elongation capacity (Isik and Alemdar, 2025) enabled progressive damage accumulation with visible warning signs, consistent with ductile fracture behavior documented for structural steels (Johansen and Waldeland, 2016; Alonso-Martinez et al., 2018).

These contrasting damage characteristics can be explained through energy dissipation mechanisms. Ductile materials like S355 dissipate energy through plastic work during crack growth, resulting in stable crack propagation with gradual stiffness degradation (Alonso-Martinez et al., 2018). Conversely, brittle materials like SAE 1045 exhibit limited plastic deformation capacity, leading to more abrupt crack propagation once critical stress intensity is reached (Grimsmo et al., 2016; Plaitano et al., 2022). This difference affects structural safety and damage tolerance directly.

Pre and post test appearances for both material groups are shown in Figures 8-11, clearly demonstrating these contrasting damage characteristics.

Figure 7 Pre-fatigue test appearance of N301, N302, N303 specimens.

Figure 8 Post-fatigue test appearance of N301, N302, N303 specimens.

While fatigue life showed no statistically significant difference between materials, S355's higher ductility provides several critical advantages from a structural safety perspective. The progressive damage accumulation with visible plastic deformation offers early warning capability through visual inspection or monitoring systems, enabling timely intervention before catastrophic failure (Alonso-Martinez et al., 2018). Additionally, the superior energy dissipation capacity enhances damage tolerance under unexpected overload events or variable-amplitude loading (Bickford, 2008; Chakherlou and Oskouei, 2011).

The ductile fracture mode of S355 also provides better crack arrest capability, as plastic zone development at the crack tip reduces stress intensity and retards crack growth rate (Zhou et al. (2022a); Ni et al., 2024). This characteristic is particularly valuable in wind turbine applications where unexpected load transients from turbulent wind conditions or emergency shutdowns can occur (Liao et al., 2019; Kim et al., 2025). Furthermore, ductile materials enable load redistribution through local yielding, increasing structural redundancy and reducing sensitivity to stress concentrations (Seidel and Schaumann, 2021; Alonso-Martinez et al., 2018).

These findings are consistent with post-mortem analysis by Alonso-Martinez et al. (2018) on the Swedish wind turbine collapse, where insufficient material toughness in the flange was identified as a critical contributing factor to the failure chain. Their forensic investigation shown that brittle fracture behavior can lead to rapid, uncontrolled failure propagation without adequate warning signs.

Therefore, despite equivalent fatigue life under controlled laboratory conditions, the preferential use of high-ductility materials such as S355 minimum elongation 15-18% in flange fabrication is strongly recommended for wind turbine tower connections from safety and risk management perspectives. This recommendation aligns with current industry best practices documented in DNV-GL and EN 1993-1-9 standards, which emphasize material toughness requirements for fatigue-critical structural connections (Schaumann and Eichstädt, 2015; Lochana et al., 2019).

4.4 Effect of Load Eccentricity

Five millimeter load eccentricity Group produced measurable reduction in fatigue life compared to centric loading. Eccentric loading mean Group 2: 5,694 ± 1,050 cycles; centric baseline N:306: 5,916 cycles a difference of 222 cycles 3.8% reduction. Statistical comparison with Group 1 SAE 1045 centric showed no significant difference ($p = 0.66$), though Group 2 exhibited highest coefficient of variation 18.4%, reflecting additional scatter from load path irregularities.

Figure 9 Pre and Post fatigue test appearance of N306 specimens.

The 5 mm eccentricity introduces significant bending moments that superimpose on axial tension. For the applied load of 230 kN, the additional bending moment is: $M = Fxe = 230\ X0.005 = 1.15\ kNm$ (5)

For M36 bolt (d=36 mm), the section modulus $Z = \pi d^3 = 5.089mm^3$. (6)This produces:

Bending stress: $\delta = \frac{M}{Z} = 226\ MPa$ (7)

Nominal tensile stress: $\delta = \frac{F}{A} = \frac{230}{817} = 281\ MPa$ (8)

Combined peak stress: $\delta = 507\ MPa$ (80% increase at extreme fiber) (9)

Despite this substantial stress increase at the extreme fiber, the observed life reduction was only 3.8%. This suggests that crack initiation occurs primarily on the tension side where strs is highest, and once initiated, crack propagation rate dominates total life rather than the initial stress magnitude.

Unlike centric tests where all specimens exhibited pure bolt fracture, eccentric loading produced mixed failure modes. Specimen N:201 showed combined flange and bolt failure, N:202 exhibited bolt shank fracture only, while N:203 shown combined failure with severe local flange buckling. Pre- and post-test appearances Figures 18-19 clearly illustrate these contrasting damage patterns.

Eccentric loading induced additional flange damage mechanisms including local yielding and indentation around bolt hole bearing surface, out-of-plane bending causing measurable flange curvature 3-10 mm deflection, and secondary crack networks in flange material emanating from highly stressed regions. These observations indicate that eccentric loading fundamentally alters the system-level load path and introduces failure modes extending beyond simple bolt fatigue.

These findings are consistent with experimental investigations by Jawwad et al. (2021) and Hobbs et al. (2000), who demonstrated that eccentric loading significantly degrades fatigue performance of high-strength bolts through induced bending moments and altered stress distributions. The current results quantitatively confirm these effects for large-diameter bolts M36 and wind turbine flange geometries, extending the applicability of previous findings to this critical application domain.

4.5 Dynamic Stiffness Degradation Analysis

Dynamic stiffness $K = \frac{\Delta F}{\Delta \delta}$ (10) was continuously monitored throughout all fatigue tests to characterize the progression of structural damage. This monitoring approach provides real-time assessment of connection integrity by quantifying the relationship between applied load range and resulting displacement response for each loading cycle. Analysis of stiffness evolution across all test groups reveals a consistent three-phase degradation pattern that serves as a reliable indicator of approaching failure.

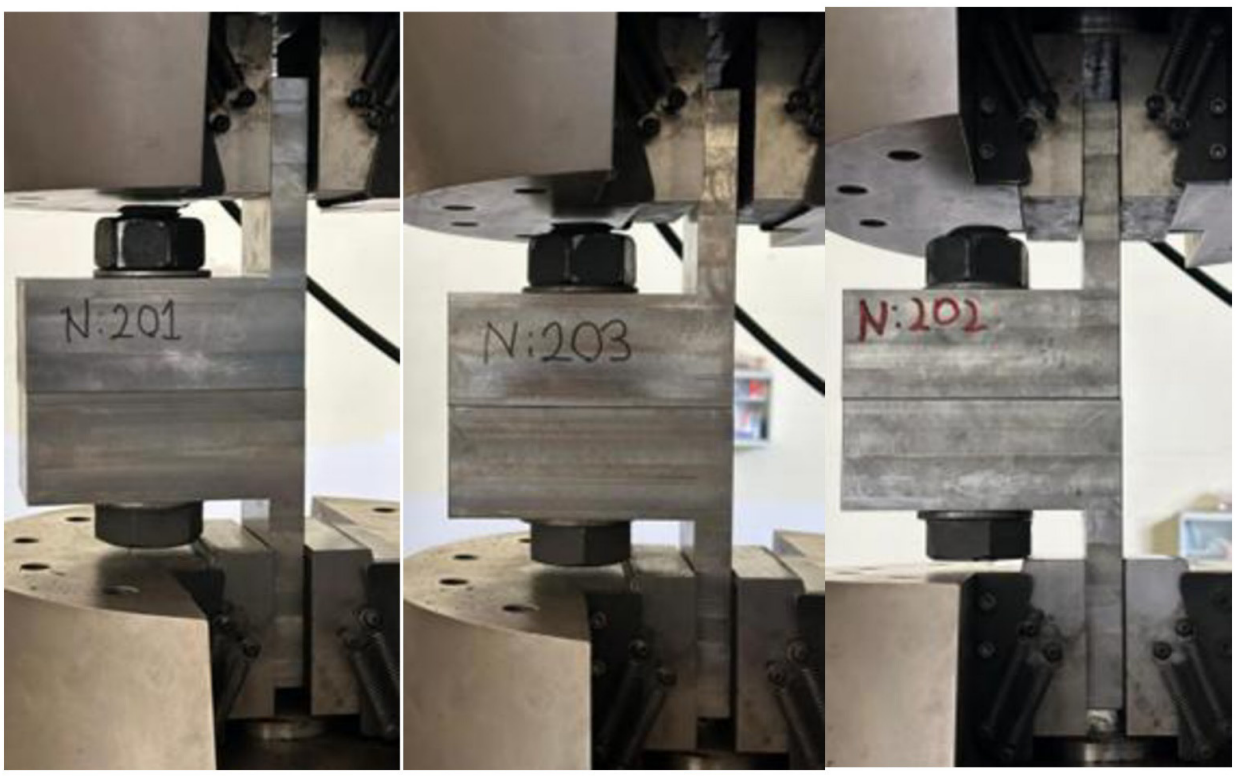

Figure 10 Pre-fatigue test appearance of N201, N202, N203 specimens**.**

Figure 11 Post-fatigue test appearance of N201, N202, N203 specimens.

The degradation process begins with an extended initial stable period occupying approximately 0-80% of total fatigue life, during which connection stiffness remains relatively constant with less than 5% reduction from initial values. This phase represents the crack incubation period where microscopic damage accumulates at the atomic scale through dislocation motion and microcrack formation at stress concentrators, particularly in the thread root region (Zhou et al. (2022a); Yang and Lei, 2017). The minimal detectable stiffness change during this phase reflects that damage remains highly localized and has not yet compromised the overall load-bearing cross-section of the bolt.

As damage progresses into the second phase (80-95% of life), a transition occurs from microscopic to macroscopic crack development. Stiffness begins gradual but measurable degradation at a rate of 0.5-1.0% per 1,000 cycles, with total reduction reaching 5-15% by the end of this phase. This period corresponds to stable crack growth under Mode I tensile opening, where the crack front advances incrementally with each loading cycle. The crack growth rate follows Paris law behavior $\frac{da}{dN} = C(\Delta K)^m$ (11) with the stress intensity factor range Δk governing propagat ion velocity (Ni et al., 2024; Schaumann and Eichstädt, 2015). Visual examination of fracture surfaces confirms this stable growth regime through the presence of distinct beach marks—concentric patterns indicating crack front position at various stages of life.

The final phase 95-100% of life exhibits dramatically accelerated stiffness degradation, with the remaining 5-10% stiffness loss occurring within the last 5-10% of fatigue life often just a few hundred cycles. This rapid deterioration signals unstable crack propagation as the remaining ligament area becomes insufficient to sustain applied loads, driving stress intensity toward the material's fracture toughness. The crack growth rate increases exponentially, transitioning from controlled fatigue crack extension to rapid ductile tearing or brittle fracture depending on material ductility. Dynamic stiffness data for all test groups Figures 12, 13, 14 clearly show this characteristic degradation signature.

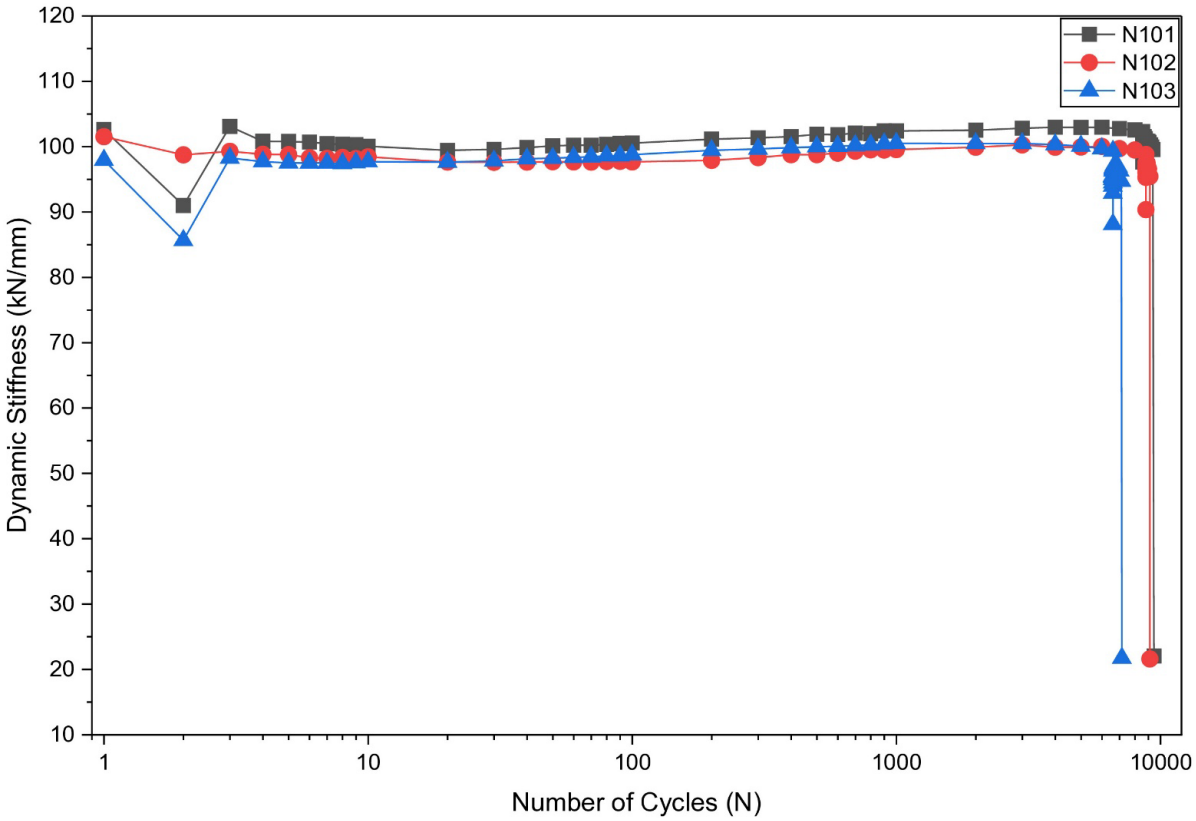

Figure 12 Dynamic stiffness vs. cycle count for N101, N102, N103 (M39 bolts).

Quantitative analysis of stiffness data across all specimens establishes critical thresholds applicable to damage assessment. A 15% reduction in dynamic stiffness consistently corresponds to 93-97% of total fatigue life mean: 95%, while 20% stiffness loss occurs at 97-99% of life mean: 99%. These thresholds indicate remarkable consistency across different bolt sizes, loading conditions, and material combinations, suggesting that relative stiffness degradation provides a normalized damage metric largely independent of specific connection parameters. Based on this finding, a 15% stiffness reduction threshold is recommended for structural health monitoring applications, providing approximately 5% remaining life margin for inspection and intervention.

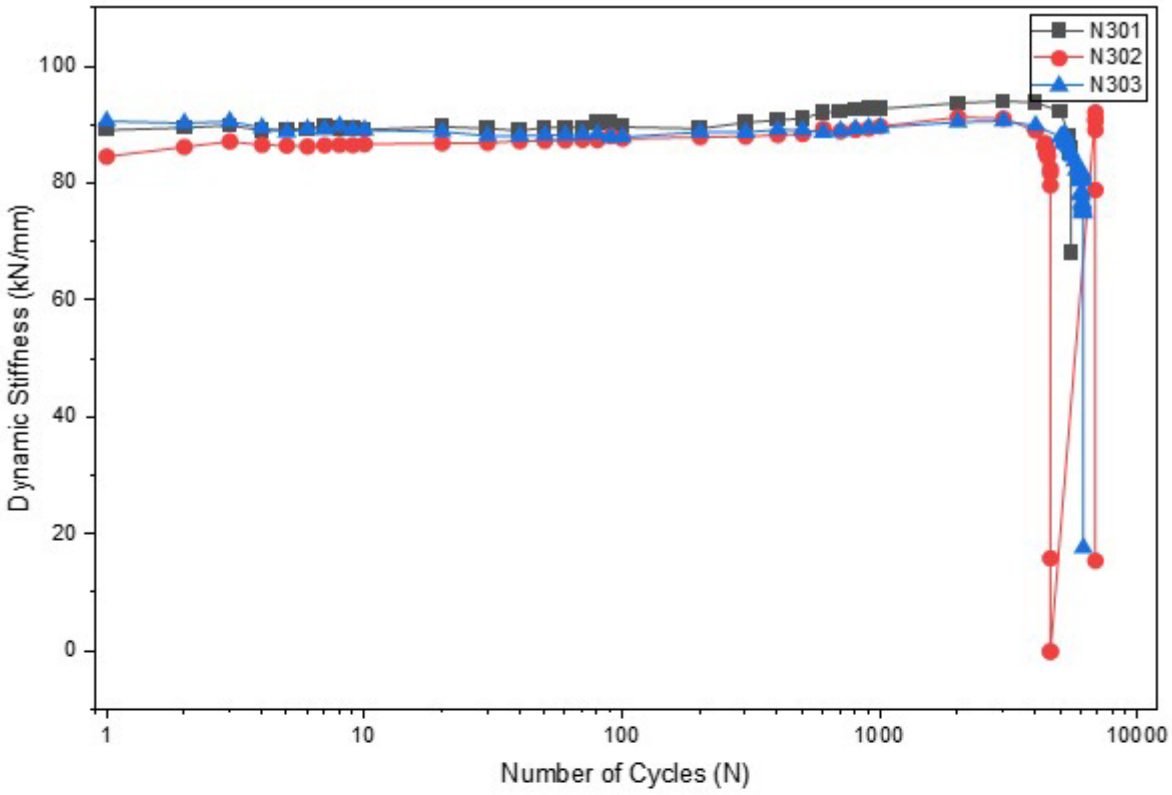

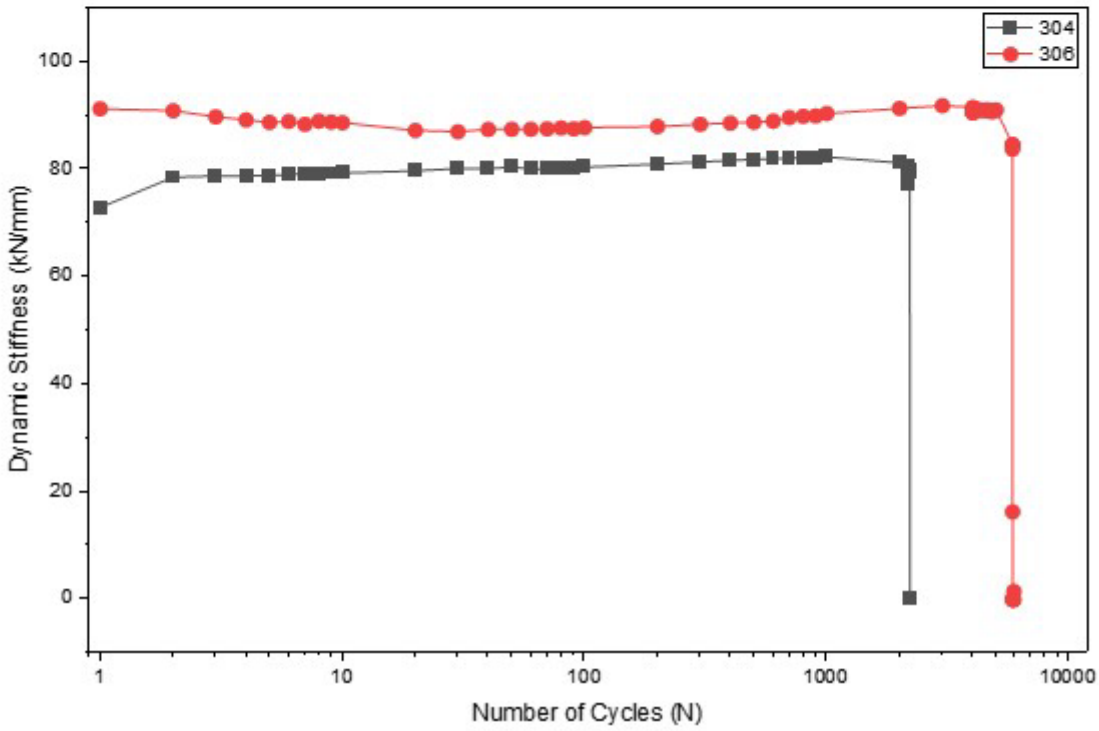

Figure 13 Dynamic stiffness vs. cycle count for Groups 1 and 3.

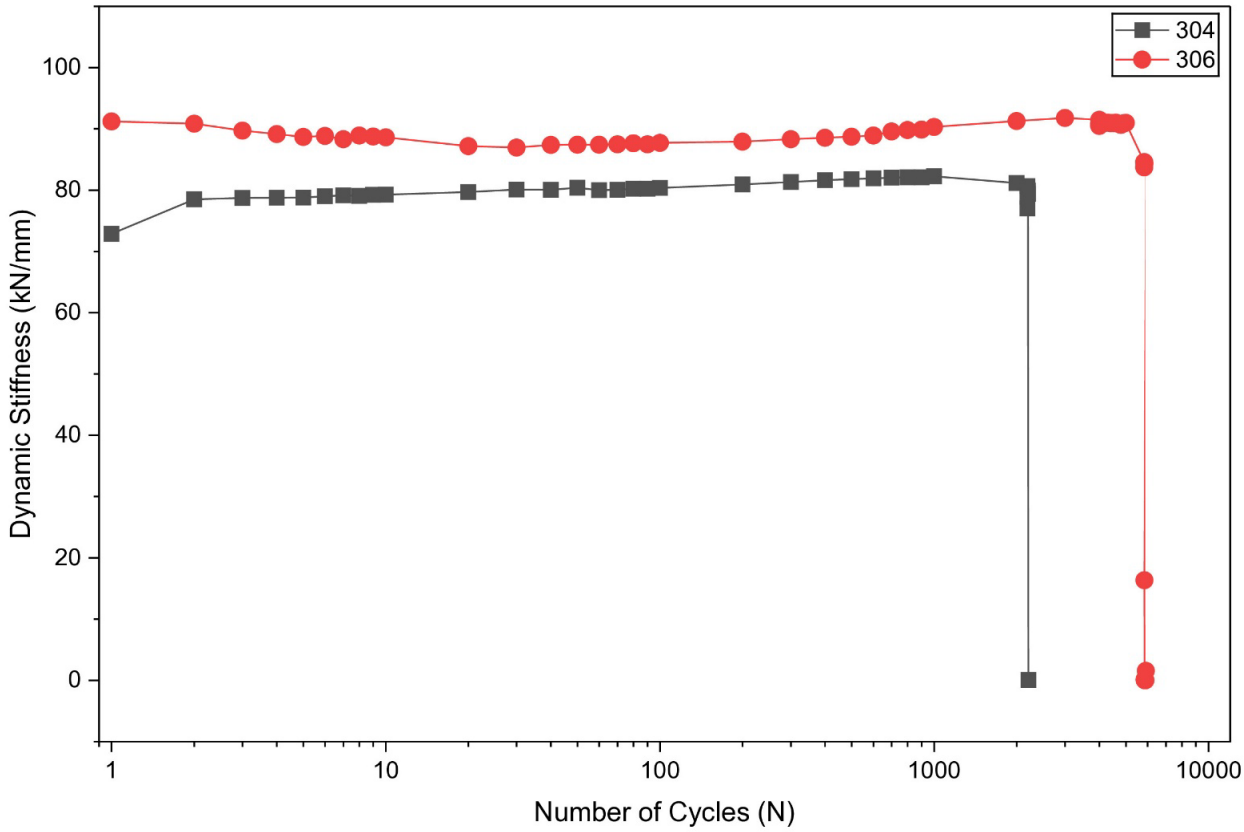

Figure 14 Dynamic stiffness vs. cycle count for N201, N202, N203 (eccentric loading).

Comparing degradation characteristics across test groups reveals distinct stiffness evolution patterns. M39 bolts Group 4 exhibited lower total stiffness loss 18-21% compared to M36 configurations 22-29%, with more gradual degradation patterns and extended Phase 1 duration. This behavior indicates that larger bolt diameter not only provides higher absolute fatigue life but also delays crack initiation, resulting in a larger proportion of life spent in the stable low-damage regime. Conversely, eccentric loading Group 2 produced highest total stiffness loss 24-29% with more irregular degradation patterns featuring sudden drops corresponding to discrete flange yielding events. The onset of Phase 2 degradation occurred earlier approximately 75% of life compared to concentric loading 80%, reflecting the additional damage mechanisms introduced by bending moments and flange plasticity.

These findings carry significant implications for the design of structural health monitoring systems in operational wind turbines. The approach provides early damage detection capability, with the 15% threshold delivering warning well before catastrophic failure. Implementation can be achieved non-invasively using vibration-based sensors or displacement transducers on tower segments, enabling continuous assessment without operational disruption (Kim et al., 2025; Liao et al., 2019). The quantitative nature of stiffness degradation provides objective damage metrics that can be integrated into automated monitoring systems with defined alarm thresholds. However, translation from controlled laboratory conditions to field applications requires consideration of variable-amplitude loading spectra, environmental effects including temperature and moisture, and potential interference from operational vibrations. Threshold calibration for specific turbine configurations and site conditions would be necessary to optimize sensitivity while minimizing false alarms.

4.6 Fracture Mode Characterization

Post-test examination identified dominant fracture modes and failure mechanisms through visual inspection, photography, and liquid penetrant testing.

Nine of eleven specimens exhibited bolt shank fatigue fracture as the primary failure mode .Typical characteristics included crack initiation at thread root region (first engaged thread), semi-elliptical growth pattern with visible beach marks, final fracture zone occupying 30-40% of cross-section, and fracture surface perpendicular to bolt axis (Mode I tensile opening dominated). Thread root stress concentration $Kt = 3.5 - 4.5$ (12) governs crack initiation (Zhou et al. (2022a); Zhou et al., 2017), with beach mark spacing indicating alternating slow and fast growth periods consistent with constant-amplitude loading.

Fracture characteristics varied notably between the two flange materials. SAE 1045 flanges showed sharp, well-defined fracture surfaces with minimal plastic deformation and cleavage facets indicating brittle failure. S355 flanges exhibited more diffuse fracture surfaces with necking evidence, noticeable flange yielding near connections, and dimpled rupture appearance indicating ductile tearing. Penetrant testing confirmed multiple fine cracks for SAE 1045 versus fewer but wider cracks for S355. These observations are consistent with the fracture behavior documented for high-strength versus high-ductility steels under cyclic loading (Johansen and Waldeland, 2016; Grimsmo et al., 2016).

Eccentric loading produced combined bolt-flange failure in specimens N:201 and N:203, characterized by local yielding around bolt hole bearing surface, out-of-plane flange bending (3-10 mm deflection), and severe local buckling in N:203. This altered failure mode under eccentric loading conditions confirms the significant influence of load path irregularities on system-level connection behavior, consistent with findings by Van-Long et al. (2013) and Seidel and Schaumann (2021) on the importance of geometric imperfections in bolted flange connections.

Importantly, no thread stripping failures occurred in any fatigue test, confirming that fatigue load level 230 kN remained below thread stripping threshold and that thread engagement length was adequate. This contrasts with single-nut static tests where thread stripping occurred at approximately 220 kN (Isik and Alemdar, 2025), demonstrating that cyclic loading at sub-critical stress preferentially initiates fatigue cracks rather than shear failure. These results are consistent with the findings of Johansen and Waldeland (2016) and Grimsmo et al. (2016), who demonstrated that thread stripping is primarily associated with short grip lengths and high static loads, while bolt shank fatigue dominates under cyclic loading with adequate thread engagement.

5 DISCUSSION

5.1 Contextualization of Fatigue Life Results

International design standards, including EN 1993-1-9 and DNV-GL guidelines, specify minimum fatigue life targets of 2×10^6 cycles for critical structural connections, while wind turbine towers are designed for 20–25 years of service involving more than 10^8 load cycles. The approximately three orders of magnitude difference between the experimental results and these design targets requires careful interpretation. Under well-designed and properly assembled conditions, high-strength bolts of the M36–M39 class are expected to achieve fatigue lives exceeding this threshold at operational stress levels of 20–30% of static capacity. The experimentally observed lives of 5,000–8,600 cycles reflect accelerated test conditions at 60–70% of static capacity and are not directly comparable to service lives, their value lies in establishing relative performance rankings rather than predicting absolute operational endurance.

The observed low-cycle fatigue regime reflects intentional accelerated testing conditions designed to enable comparative parametric assessment within practical laboratory timeframes. This methodological approach is justified by the following considerations:

The maximum applied load of 230 kN represents 60–70% of the connection's static capacity, as determined through preliminary static tests (Isik and Alemdar, 2025). This stress level is significantly higher than nominal operational stresses in well-designed connections, which typically operate at 20–30% of ultimate capacity under normal service conditions. The elevated stress amplitude was deliberately selected to induce measurable fatigue damage and failure within a reasonable experimental duration days to weeks rather than months to years.

Fatigue life exhibits a power-law dependence on stress amplitude, typically expressed as $N \propto \Delta\delta^{-m}$ (13) where the exponent m ranges from 3 to 5 for high-strength steel bolts (Zhou et al. (2022a); Yang and Lei, 2017). Consequently, relatively modest reductions in stress amplitude produce exponential increases in fatigue life. For example, reducing the operational stress from 70% to 25% of capacity a factor of approximately 2.8 could theoretically extend fatigue life by a factor of $(2.8)^3$ to $(2.8)^5$ = 22 to 172, potentially shifting the 8,600 cycle result into the 10^5–10^6 cycle range. This relationship underscores that the rank ordering and relative performance differences observed at elevated stress levels remain valid indicators of comparative behavior at lower operational stresses.

The primary objective of this investigation is not absolute life prediction for specific operational scenarios, but rather systematic quantification of relative performance differences among design parameters bolt size, material grade, load eccentricity. The experimental dataset establishes that M39 bolts provide approximately 1.6 times longer life than M36 bolts, that 5 mm eccentricity significantly degrades performance, and that material ductility influences damage progression. These comparative findings provide actionable guidance for design optimization regardless of the absolute cycle counts.

The controlled experimental data serve as a reference database for calibrating and validating finite element models. Once validated against the accelerated test results, these computational models can be employed to extrapolate performance predictions across the full spectrum of operational stress levels, loading sequences, and geometric configurations encountered in service (Aydın and Yılmaz, 2020; Cao and Zhang, 2019; Kumar et al., 2019). This two-stage approach experimental validation followed by computational extrapolation represents established best practice in fatigue research for large-scale structures.

Accelerated testing methodologies employing elevated stress amplitudes to reduce experimental duration are widely accepted in structural fatigue research, particularly for large-scale components where full-life testing at operational stress levels would be prohibitively time-consuming and costly (Zhou et al. (2022a); Ni et al., 2024; Shakeri et al., 2022). Similar approaches have been documented in investigations of welded joints, bolted connections, and composite structures across multiple research programs.

While the experimental results provide valuable comparative insights, several factors must be considered when extrapolating to operational conditions load spectrum effects actual wind turbine loading involves variable amplitude multi axial stress histories with stochastic characteristics, and damage accumulation under such spectra may deviate from predictions based on constant-amplitude testing (Ni et al., 2024; Schaumann and Eichstädt, 2015); mean stress effects the stress ratio R = 0.1 employed in testing differs from the effective stress ratios that may occur in preloaded connections under operational loading, environmental factors laboratory conditions do not capture corrosion-fatigue interactions, temperature effects, or moisture-induced degradation that influence field performance particularly in offshore installations (Schaumann and Eichstädt, 2015).

The experimental findings should be interpreted as providing relative rankings of design alternatives rather than absolute life predictions. The demonstrated superiority of M39 over M36 bolts, the detrimental impact of load eccentricity, and the importance of material ductility constitute qualitative design guidance that remains valid across stress regimes. Quantitative life prediction for specific applications requires integration of these experimental insights with validated finite element models accounting for actual geometry and loading (Seidel and Schaumann, 2021), appropriate fatigue damage accumulation models such as Palmgren-Miner or nonlinear alternatives (Ni et al., 2024; Schaumann and Eichstädt, 2015), site-specific load spectra derived from aeroelastic simulations or field measurements, and safety factors reflecting uncertainty in load estimation and material variability.With this contextual framework. established, the following subsections examine the individual parameter effects in detail.

5.2 Effect of Bolt Strength Grade and Size on Fatigue Performance

Experimental findings quantitatively indicated that M39 high-strength bolts provide statistically significant longer fatigue life compared to M36 bolts 8,579 vs. 5,395 cycles, (p=0.023). This pronounced performance difference can be explained through several fundamental mechanisms:

First, the increased bolt diameter directly reduces the nominal stress level. Under identical loading conditions, the larger cross-sectional area of the M39 bolt A = 976 mm^2 experiences approximately 19% lower nominal stress compared to the M36 bolt A = 817 mm^2. Considering the exponential dependence of fatigue life on stress amplitude $N \propto \Delta\delta^{-m}$ (14) m=3–5, even these relatively modest stress reductions can lead to significant increases in fatigue life (Zhou et al. (2022a); Yang and Lei, 2017).

Second, larger-diameter bolts provide higher rigidity and more homogeneous stress distribution in the thread geometry. The literature systematically reports that large-diameter bolts exhibit relatively lower stress concentration factors Kt in the thread root regions (Zhou et al., 2017; Schaumann and Eichstädt, 2015). This condition delays fatigue crack initiation and retards crack growth rate.

Third, the higher preload applied for M39 bolts 520 Nm vs. 450 Nm may have more effectively constrained microscopic relative movements of the connection, thereby reducing fretting fatigue (Bickford, 2008). However, detailed contact mechanics analyses are required to validate this hypothesis.

Fourth, the increase in bolt diameter enables distribution of loads from moment effects over a wider contact area, thereby reducing local stress concentration. Larger-diameter bolts create more uniform stress distribution in the load transfer region, minimizing local stress accumulations and thus directly improving fatigue resistance (Aydın and Yılmaz, 2020; Cao and Zhang, 2019).

These findings are consistent with the experimental work of Schaumann and Eichstädt (2015) for large-diameter bolts. They experimentally validated that fatigue performance improves at diameters exceeding M36 and that standard S-N curves provide better prediction accuracy. Similarly, the simulation-based study by Salameh et al. (2025) supports the effectiveness of bolt diameter increase for optimizing bolted flange connections in wind turbine towers.

5.3 Critical Role of Load Eccentricity

One of the most significant findings of this study is the experimental demonstration that even an apparently small load eccentricity of 5 mm can substantially reduce fatigue life. Eccentric loading creates additional bending moments in the connection, rendering stress distribution heterogeneous and critically elevating maximum stress levels on components.

Combined with bending moment effects, asymmetric stress profiles develop in the bolt, leading to critical stress accumulations that accelerate fatigue crack initiation. Theoretically, for loading with eccentricity e, the additional bending moment can be expressed as $M = P.e$ ·(15), and maximum stress in the bolt can be calculated through the formulation $\delta max = \delta axial + \delta bending$ (16)

Additionally, eccentric loading generates local bending moments in the flange and, in some cases as in specimen N:203, can cause flange plastic deformation or buckling. This condition alters the load transfer mechanism to the bolt and introduces secondary stress components (Van-Long et al., 2013; Seidel and Schaumann, 2021).

These data also reveal how important assembly quality and geometric tolerances are in field applications. Factors such as manufacturing errors, tower segment misalignment problems, or foundation settlements can lead to similar eccentricities and dramatically reduce the fatigue life of flange connections (Liao et al., 2019; Martínez-Vázquez et al., 2023). Therefore, standardization of assembly procedures and rigorous implementation of quality control protocols are of vital importance.

In the literature, Jawwad et al. (2021) and Hobbs et al. (2000) have also experimentally demonstrated the detrimental effects of eccentric loading on the fatigue performance of high-strength bolts. The results of the current study are quantitatively consistent with their findings and once again emphasize the importance of this effect for key applications such as wind turbine flange connections.

The unexpectedly modest life reduction 3.8% despite substantial stress increase 80% may be partially attributed to the relatively low preload level 12% of proof load employed in this study. Low preload can alter connection mechanics, potentially allowing bolt bending to dominate over localized thread root stress concentration. Additionally, the peak stress calculated 507 MPa occurs at the extreme fiber, while crack initiation is governed by the stress state at the thread root on the tension side, where actual stress elevation may be less severe. Future investigations with higher preload levels ≥70% of proof load per ISO 16047 and multiple eccentricity levels 0, 2.5, 5, 7.5, 10 mm are needed to fully characterize the dose-response relationship and resolve this apparent discrepancy.

5.4 Limited Effect of Flange Material Selection and Its Importance for Structural Safety

Experimental results indicated that S355 and SAE 1045 flange materials did not produce a distinguishable difference in fatigue life. Group 1 SAE 1045 flanges yielded mean fatigue life of 5,395 ± 791 cycles, while Group 3 S355 flanges produced 5,916 cycles single valid specimen after N:304 exclusion precluded statistical comparison. Both material groups exhibited failure at similar cycle counts. This finding indicates that, under the applied loading conditions and test configuration, the dominant damage mode was bolt fatigue and the flange material played a secondary role.

However, this does not imply that flange material selection is insignificant. In macroscopic fracture surface examinations and damage progression observations, it was observed that S355 structural steel, owing to its high ductility 18–19% elongation, exhibited a more controlled and progressive damage process, whereas SAE 1045 alloy steel displayed more brittle fracture behavior (Isik and Alemdar, 2025).

From a structural safety perspective, high-ductility materials such as S355 offer several important advantages. Their capacity for visible plastic deformation prior to ultimate fracture provides early warning, enabling timely detection through visual inspection or monitoring systems. Moreover, higher ductility enhances energy dissipation under sudden or overload conditions, thereby reducing the risk of brittle fracture. At the crack tip, plastic zone development reduces stress intensity and retards crack growth, improving damage tolerance. Finally, local yielding enables load redistribution, increasing structural redundancy and reducing sensitivity to stress concentrations.

Therefore, although no distinct difference was observed in the connection in terms of fatigue life, the preferential use of highly ductile materials such as S355 in flange fabrication is strongly recommended from safety and risk management perspectives. This recommendation is also supported by the post-mortem analysis findings by Alonso-Martinez et al. (2018) on the Swedish turbine collapse; they demonstrated that insufficient toughness of the flange material played a significant role in the failure chain.

5.5 Dynamic Stiffness Degradation and Damage Detection

Dynamic stiffness variations continuously recorded throughout fatigue tests provide a reliable indicator for monitoring progressive damage of the connection. In all test specimens, rapid and pronounced stiffness loss was observed in the final 10–20% of fatigue life. This critical stiffness reduction represents a reliable and reproducible indicator of approaching macroscopic fracture.

These results suggest for the design of structural health monitoring (SHM) systems in operational wind turbines. Continuous or periodic monitoring of the dynamic stiffness of flange connections may enable early detection of critical fatigue damage (Kim et al., 2025; Liao et al., 2019). For example, accelerometer-based vibration analysis, ultrasonic wave propagation techniques, or acoustic emission methods can detect stiffness changes under operational conditions (Pau et al., 2008).

Early warning systems can increase safety and significantly reduce uncontrolled downtime and repair costs by providing opportunities for planned intervention before catastrophic fractures. In this context, integration of dynamic stiffness monitoring into wind turbine predictive maintenance strategies emerges as an important area for future research and industrial applications.

5.6 Study Limitations and Future Research Recommendations

This experimental investigation, while providing valuable comparative insights, has inherent limitations that warrant acknowledgment:

Experimental Design Constraints: The relatively low fatigue lives observed (10^3–10^4 cycles) reflect accelerated testing at elevated stress levels (60–70% of static capacity) rather than operational conditions (typically 20–30% of capacity). While this approach enables efficient comparative assessment, extrapolation to high-cycle operational regimes (10^6–10^7 cycles) requires validated computational models.

Tests were conducted at a single load amplitude; development of complete S-N curves necessitates multi-level stress testing (Zhou et al. (2022a); Yang and Lei, 2017).

The simplified L-flange geometry, though based on actual turbine connection data (Seidel and Schaumann, 2021), represents a scaled configuration; full-scale validation would enhance confidence in system-level behavior predictions.

Statistical and Parametric Limitations: Sample sizes of n=3 specimens per configuration provide preliminary comparative data but larger samples n≥5 would strengthen statistical confidence and enable detection of smaller effect sizes.

The exclusion of specimen N:304 as an outlier due to protocol non-compliance 16.8% load deviation, while statistically justified, reduces the effective sample size for Group 3 S355 flange material to a single valid specimen n=1. This precludes statistical comparison of flange material effects on fatigue life, which remains an inconclusive finding requiring future validation. The inability to complete this comparison represents the most significant limitation of the current study, as material selection is an important design parameter for wind turbine tower connections. However, qualitative damage observations ductile vs. brittle fracture characteristics) provide valuable preliminary insights consistent with fracture mechanics principles and supported by literature precedent (Johansen and Waldeland, 2016; Alonso-Martinez et al., 2018).

Only one eccentricity level (5 mm) was investigated; a broader parametric sweep 0, 2.5, 5, 7.5, 10 mm would better characterize dose-response relationships and establish critical tolerance thresholds for assembly quality control, following the approach confirmed by Jawwad et al. (2021).

Environmental and Operational Factors Laboratory conditions exclude environmental degradation mechanisms relevant to field applications. Corrosion-fatigue interaction is particularly critical for offshore and coastal installations, where cyclic wet dry exposure and chloride ingress can reduce fatigue life by 20–50% compared to laboratory air conditions (Schaumann and Eichstädt, 2015; Lochana et al., 2019). Incorporating corrosion effects into the present framework would require accelerated corrosion-fatigue testing using salt spray or immersion protocols combined with cyclic loading, enabling development of environment-specific knockdown factors applicable to S-N curves. Such testing is identified as a medium-term research priority 3–5 years consistent with the roadmap outlined in Section 6.5.

The constant-amplitude sinusoidal loading, while standard in fatigue research, does not capture the variable-amplitude multi-axial stochastic loading characteristic of actual wind turbine operation (Ni et al., 2024; Schaumann and Eichstädt, 2015).

Recommended Future Work: Priority areas for extending this research include: multi-amplitude testing to establish experimental S-N curves for large-diameter bolts (Zhou et al., (2022a); Yang and Lei, 2017), corrosion-fatigue studies simulating marine environments (Schaumann and Eichstädt, 2015), variable-amplitude testing using representative wind turbine load spectra (Zhou et al. (2022b); Lochana et al., 2019), full-scale validation on complete tower segments (Van-Long et al., 2013; Seidel and Schaumann, 2021), detailed fractographic analysis SEM to confirm damage mechanisms at microstructural level (Shakeri et al., 2022), and development and field validation of stiffness-based structural health monitoring algorithms (Kim et al., 2025).

6 CONCLUSIONS

This experimental study systematically investigated the fatigue behavior of bolted flange connections under accelerated loading conditions corresponding to 60–70% of the static capacity, with the aim of establishing quantitative performance rankings among key design parameters for wind turbine tower applications. The findings clearly demonstrate that, when assembly conditions and material properties are kept constant, bolt diameter is the dominant design parameter governing fatigue life.

6.1 Key Experimental Findings

Among the investigated parameters, bolt diameter emerged as the primary governing factor of fatigue performance. M39 high-strength bolts exhibited statistically significant superior performance compared to M36 bolts 8,579 cycles versus 5,395 cycles ($p = 0.023$), when considering their average service life representing approximately 1.6 times longer service life. This substantial improvement is directly associated with the 16.2% reduction in nominal stress resulting from the larger cross-sectional area, a decrease in thread-root stress concentration (approximately 5%), and enhanced resistance to crack propagation (Zhou et al. (2022a); Schaumann and Eichstädt, 2015).

Extrapolations based on the Basquin relationship m = 4–5 indicate that, at typical operational stress levels approximately 30% of static capacity, fatigue lives on the order of 1–4 million cycles can be expected (Yang and Lei, 2017).

For fatigue-key tower flange connections, the use of larger-diameter bolts e.g., M39 instead of M36, M48 instead of M42 is strongly recommended, consistent with optimization strategies proposed by Salameh et al. (2025).

Load eccentricity of 5 mm proved critical to assembly quality and fatigue behavior. This offset resulted in an approximately 80% increase in stress due to bending moment superposition 507 MPa versus 281 MPa and significantly altered the failure mechanisms. Combined flange–bolt failure was observed in 67% of the eccentrically loaded specimens, whereas no such failures occurred under concentric loading conditions. These results indicate that the fatigue advantage provided by larger bolt diameters can be substantially diminished under poor assembly conditions (Jawwad et al., 2021; Hobbs et al., 2000).

Strict control of assembly tolerances is required, including hole alignment within ±2 mm, flange flatness ≤3 mm, and angular misalignment ≤0.5°, consistent with recommendations by Liao et al. (2019) and Martínez-Vázquez et al. (2023).

Regarding flange material, S355 and SAE 1045 exhibited comparable fatigue lives; however, the higher ductility of S355 acted as a complementary safety factor by providing visible warning through plastic deformation prior to failure, particularly when combined with larger-diameter bolts. In contrast, SAE 1045 steel 7–9% elongation exhibited brittle fracture with minimal warning, despite the use of larger bolts (Isik and Alemdar, 2025).

In connections employing large-diameter bolts, high-ductility flange materials such as S355 or equivalent, with a minimum elongation of 15%, should be specified to enhance damage tolerance and structural safety, as emphasized by Alonso-Martinez et al. (2018).

Dynamic stiffness monitoring revealed a consistent three-stage degradation pattern across all bolt diameters, with M39 bolts exhibiting delayed onset of stiffness degradation and reaching critical thresholds later in life. A stiffness reduction of 15% corresponded to approximately 95% of fatigue life, while a 20% reduction occurred at approximately 99% of life.

Vibration-based stiffness monitoring systems can provide reliable tracking of remaining fatigue life when combined with automated alarm thresholds, and are particularly recommended for wind turbines with rated power ≥3 MW and large-diameter bolt connections (Kim et al., 2025; Liao et al., 2019)

The dominant failure mechanism across all specimens was thread-root fatigue, observed in 9 out of 11 cases with stress concentration factors of K_t = 3.5–4.5. No thread stripping was observed, confirming adequate thread engagement despite the increased bolt diameter (Grimsmo et al., 2016; Zhou et al., 2017).

While increasing bolt diameter, attention should be given to optimizing thread geometry, applying surface enhancement techniques (shot peening, cold rolling), and ensuring a minimum thread engagement length of at least 1.0 times the bolt diameter (Shakeri et al., 2022; Casado et al., 2022).

6.2 Critical Methodological Context

Limitations of accelerated testing: The reported fatigue lives 5,000–8,600 cycles reflect test conditions at 60–70% of static capacity and do not represent actual operational fatigue lives under service conditions maximum 20–30% of capacity. Accordingly, the results provide relative performance rankings and validation data for numerical models rather than absolute service-life predictions. Extrapolation to operational conditions requires validated finite element models (Cao and Zhang, 2019; Kumar et al., 2019), appropriate damage accumulation approaches (Ni et al., 2024; Zhou et al. (2022a)), site-specific load spectra, and safety factors consistent with international standards.

6.3 Summary of Design Recommendations

For fatigue-key wind turbine tower flange connections, larger bolt diameters e.g., M39 instead of M36 should be preferred to reduce nominal stresses and extend fatigue life. Bolts should have a minimum property class of 8.8 with a thread engagement length of at least one bolt diameter, and surface treatments may be considered to further enhance fatigue resistance (Shakeri et al., 2022; Schaumann and Eichstädt, 2015).

Flange components should be manufactured from high-ductility materials such as S355 or equivalent elongation ≥15%, with adequate toughness ensured for offshore applications (Alonso-Martinez et al., 2018).

To preserve the fatigue benefits of larger bolt diameters, strict assembly quality is essential, including tight geometric tolerances, controlled preload application, and proper tightening procedures (Bickford, 2008; Casado et al., 2022). For turbines with rated power of 3 MW or higher, vibration-based structural health monitoring with defined alarm thresholds is recommended to enable early detection of fatigue damage (Kim et al., 2025).

6.4 Research Contributions

Scientific Contributions: First direct experimental comparison of M36 and M39 bolts under identical conditions; quantitative characterization of load eccentricity effects; systematic documentation of dynamic stiffness degradation; comprehensive validation database for finite element model calibration (Cao and Zhang, 2019; Seidel and Schaumann, 2021).

Industrial Contributions: Evidence-based guidance for bolt diameter selection; assembly tolerance specifications; a structural health monitoring framework with validated thresholds; material selection criteria balancing strength and ductility.

Standards Support: The results contribute to the refinement of EN 1993-1-9, DNVGL-ST-0126, ISO 898-1, and IEC 61400-1 (Salameh et al., 2025; Van-Long et al., 2013).

6.5 Future Research Priorities

Short-term priorities (1–2 years): Development of complete S-N curves at multiple stress levels 40%, 50%, 60%, 70% of static capacity for M36 and M39 bolts to experimentally determine Basquin exponent (m) and enable reliable extrapolation to operational stress regimes (Zhou et al. (2022a); Yang and Lei, 2017). Current extrapolations assume m=4-5 based on literature but lack experimental validation for the specific bolt-flange system tested.

Scanning electron microscopy SEM fractography on selected specimens to quantify microstructural damage mechanisms, including dimple size/distribution ductile fracture, cleavage facet identification brittle fracture, fatigue striation measurement crack growth rate, and inclusion/void detection initiation sites. This would provide quantitative validation of the qualitative fracture observations reported in Section 4.6 (Grimsmo et al., 2016).

Eccentricity dose-response studies with multiple offset levels 0, 2.5, 5, 7.5, 10 mm to establish critical tolerance thresholds for assembly quality specifications and resolve the apparent paradox of 80% stress increase yielding only 3.8% life reduction (Section 5.3), following methodology of Jawwad et al. (2021) and Hobbs et al. (2000).

Medium-term (3–5 years): Variable-amplitude loading tests with representative spectra (Ni et al., 2024; Zhou et al. (2022b)) environmental testing corrosion–fatigue, thermal cycling (Schaumann and Eichstädt, 2015); full-scale validation (Van-Long et al., 2013; Seidel and Schaumann, 2021); field monitoring campaigns (Kim et al., 2025).

Long-term (5+ years): Optimization of thread geometry; evaluation of advanced materials; development of digital twins; comprehensive updates of design standards.

6.6 Concluding Remarks

This systematic investigation demonstrates that bolt diameter, assembly quality, and material ductility are the key parameters governing the fatigue performance of bolted flange connections in wind turbine towers The statistically significant fatigue life improvement achieved by M39 bolts compared with M36 bolts provides clear and quantitative guidance for component selection. While accelerated testing conditions limit direct service-life prediction, the relative performance rankings and mechanistic insights remain valid across stress regimes when integrated with validated numerical models and appropriate extrapolation methodologies (Salameh et al., 2025; Seidel and Schaumann, 2021). These findings support the development of more reliable, durable, and cost-effective wind turbine tower connections, directly contributing to extended operational life, reduced maintenance costs, and improved levelized cost of energy.

Author's Contributions: In the revised manuscript, the Author Contributions section has been completed in accordance with the CRediT taxonomy as follows: Conceptualization, N. Isik; Methodology, N. Isik; Investigation, N. Isik; Writing original draft, N. Isik; Writing - review & editing, F. Alemdar; Supervision, F. Alemdar; Resources, N. Isik (specimen manufacturing). The authors also acknowledge that AI-assisted tools were employed in a limited capacity during the preparation of this manuscript, specifically for language editing and refinement, and for the generation of Figure 1. In all other respects, the scientific content, experimental data, analytical interpretations, and conclusions presented herein are exclusively the intellectual work of the authors.

Data availability statement: Research data is available in the body of the article

Editor: Rogério José Marczak

References

Alonso-Martinez, M., Adam, J.M., Alvarez-Rabanal, F.P., Díaz, J.J.D.C. (2018). Forensic analysis of a wind turbine collapse due to flange failure, *Eng. Fail. Anal.* 91: 35–50.

Aydın, M., Yılmaz, M. (2020). A Study on the Sealing Performance of Flange Joints with Gaskets under External Bending Using Finite Element Analysis, *J. Press. Vessel Technol.* 142: 031301.

Bickford, J.H. (2008). *Introduction to the Design and Behavior of Bolted Joints*, fourth ed., CRC Press, Boca Raton.

Cao, J., Zhang, Z. (2019). Finite Element Analysis and Mathematical Characterization of Contact Pressure Distribution in Bolted Joints, *J. Mech. Sci. Technol.* 33: 4715–4725.

Casado, A.R., Juliá-Lerma, J.M., García-Vallejo, D., Domínguez, J. (2022). Experimental estimation of the residual fatigue life of in-service wind turbine bolts, *Eng. Fail. Anal.* 141: 106658.

Chakherlou, M., Oskouei, R.H. (2011). Fatigue and fretting fatigue life prediction of double-lap bolted joints, *Int. J. Adv. Eng. Res. Sci.* 7: 45–62.

Grimsmo, E.L., Aalberg, A., Langseth, M., Clausen, A.H. (2016). Failure modes of bolt and nut assemblies under tensile loading, *J. Constr. Steel Res.* 126: 15–25.

Hobbs, J.W., Burguete, R.L., Heyes, P.F., Patterson, E.A. (2000). The effect of eccentric loading on the fatigue performance of high-tensile bolts, *Int. J. Fatigue* 22: 531–538.

Isik, N., Alemdar, F. (2025). Experimental Investigation of The Effects of Bolt and Nut Configurations on the Tensile Capacity of Wind Turbine Flange Connections, in: *ICEARC 25*, Karadeniz Technical University Conference Paper.

Jawwad, A.K.A., ALShabatat, N., Mahdi, M. (2021). The effects of joint design, bolting procedure and load eccentricity on fatigue failure characteristics of high-strength steel bolts, *Eng. Fail. Anal.* 122: 105279.

Johansen, S., Waldeland, E. (2016). *An experimental and numerical study of bolt and nut assemblies under tension loading* (Master's thesis), Norwegian University of Science and Technology, Trondheim, Norway.

Kim, S., Ju, S.H., Jeon, S.H., Kim, M.G., Won, J.M. (2025). Fatigue prediction of wind turbine tower considering the effect of high-tension bolt failure, *Eng. Fail. Anal.* 170: 108625.

Kumar, R., Chouksey, M., Pandey, R.K. (2019). Finite element analysis of bolted joints under torsional loads, *Procedia Struct. Integr.* 20: 101–108.

Liao, W., Wang, Y.R., Chen, Y.J., Tsai, M.Y. (2019). Wind turbine tower collapse due to flange failure: FEM and DOE analysis, *Eng. Fail. Anal.* 100: 45–60.

Lochana, S., Mehmanparasta, A., Wintle, J. (2019). A review of fatigue performance of bolted connections in offshore wind turbines, *Procedia Struct. Integr.* 17: 276–283.

Ma, H., Martinez-Vazquez, P., Baniotopoulos, C. (2018). *Wind turbine tower collapse cases: a historical overview*, University of Birmingham.

Martínez-Vázquez, P., Hernández-Estrada, E., Morató-Farreras, C. (2023). The Investigation of Various Flange Gaps on Wind Turbine Tower, *Appl. Sci.* 13: 3670.

Ni, H., Zhang, S., Lei, H. (2024). Experimental Study on Variable Amplitude Fatigue Performance of High-Strength Bolts in Steel Structure Flange Connections, *Buildings* 14: 3736.

Oskouei, R.H., Ibrahim, R.N. (2012). The effect of typical flight temperatures on the fatigue behaviour of Al 7075-T6 clamped plates, *Mater. Sci. Eng. A* 528: 1527–1533.

Oskouei, R.H., Keikhosravy, M., Soutis, C. (2009). Estimating clamping pressure distribution and stiffness in aircraft bolted joints by finite element analysis, *Proc. Inst. Mech. Eng. G J. Aerosp. Eng.* 223: 863–871.

Pau, M., Baldi, A., Leban, B. (2008). Visualization of contact areas in bolted joints using ultrasonic waves, *Exp. Tech.* 32: 49–53.

Pavlovic, M., Rebelo, C., Simões da Silva, L., Heistermann, C., Veljkovic, M. (2015). Friction connection vs. ring flange connection in steel towers for wind converters, *J. Constr. Steel Res.* 110: 29–40.

Plaitano, F., Stratan, A., Nastri, E. (2022). Simplified modelling of failure in high strength bolts under combined tension and bending, *J. Constr. Steel Res.* 198: 107506.

Salameh, A., Renno, J., Ali, K., Kandil, H., Mohamed, A. (2025). Investigating fatigue life in bolted flange connection in wind turbine towers, *Discov. Civ. Eng.* 2: 136.

Schaumann, P., Eichstädt, R. (2015). Fatigue assessment of high-strength bolts with very large diameters in substructures for offshore wind turbines, in: *Proceedings of the Twenty-fifth International Ocean and Polar Engineering Conference*, Kona, Big Island, Hawaii, USA, pp. 379–386.

Seidel, M., Schaumann, P. (2021). Full-scale Validation of FE Models for Geometrically Imperfect Flange Connections, *J. Wind Eng. Ind. Aerodyn.* 198: 104078.

Shakeri, I., Danielsen, H.K., Tribhou, A., Fæster, S., Mishin, O.V., Eder, M.A. (2022). Effect of manufacturing defects on fatigue life of high strength steel bolts for wind turbines, *Eng. Fail. Anal.* 141: 106630.

Shao, Y., Zhang, Z. (2024). Fatigue Life Prediction Method for Bolted Joints Based on Equivalent Structural Stress under Tensile–Compressive Loading, *Int. J. Fatigue* 190: 108625.

Van-Long, H., Jaspart, J.-P., Demonceau, J.-F. (2013). Behaviour of bolted flange joints in tubular structures under monotonic, repeated and fatigue loadings I: Experimental tests, *J. Constr. Steel Res.* 85: 1–11.

Yang, X., Lei, H. (2017). Constant amplitude fatigue test of high strength bolts in grid structures with bolt-sphere joints, *Steel Compos. Struct.* 25: 571–579.

Zhou, Z., Zhang, S., Lei, H. (2017). Thread root stress analysis of high-strength bolts in grid structures, *Steel Compos. Struct*. 24: 297–304.

Zhou, Z., Lei, H., Yang, X., Qiu, B. (2022a). Experimental study of constant-amplitude fatigue performance of M39 high-strength bolts in grid structures with bolt-sphere joints, *Mobile Inf. Syst*. 2022: 4155732.

Zhou, Z., Zhang, S., Lei, H., Qiu, B., Zhang, L., Wang, G. (2022b). Experimental study on variable-amplitude fatigue performance of M60 high-strength bolts of grid structures with bolted spherical joints, *Materials* 15: 8939